Mechanical behaviour of granite. A compilation, analysis and correlation of data from around the world

Nathalie Domede, Thomas Parent, Alain Sellier

Mechanical behaviour of granite. A compilation, analysis and correlation of data from around the world

Domede N.*, Parent T.*, Sellier A.*

*Université de Toulouse; UPS, INSA; LMDC (Laboratoire Matériaux et Durabilité des Constructions); 135, avenue de Rangueil; F-31 077 Toulouse Cedex 04, France

Corresponding author: Nathalie DOMEDE
nathalie.domede@insa-toulouse.fr

Abstract

Granite is a building material used in old masonry structures. The aim of the work presented here is to help engineers and researchers in their choice of the mechanical parameters used to calculate these structures. A database was compiled from the international literature published between 1965 and 2016 and new tests on granite from southern France were added to it. From all these experimental results obtained with 178 different granites, the mechanical behaviour of the granites in compression and tension was analysed. Considerable variability was observed in the measured parameters, except for the bulk density. The cracking and damage thresholds of granite were estimated with respect to its compressive strength. Correlation relationships between the physical parameters of granite (bulk density, porosity, ultrasonic P-wave velocity) and its basic mechanical parameters (compressive strength, tensile strength, Young's modulus, Poisson's ratio) are proposed with a 90% confidence interval.

Keywords
Granite, mechanical behaviour, crack, strength, ultrasonic velocity

1. Introduction

This article focuses on granite considered as a construction material in masonry structures, particularly old ones such as bridges, lighthouses and monasteries. To assess the serviceability of these existing monuments, a variety of calculation methods can be used. They all need the mechanical characteristics of the materials as input. The aim of the work presented here is to help engineers and researchers to choose the mechanical parameters to be used in the calculation of masonry structures made of granite blocks.

The shortest list of parameters that have to be known includes the bulk density (ρ), Young's modulus (E), Poisson's ratio (ν), compressive and tensile strengths (f_c, f_t), and strains at peak compression (ε_{peak}). In the case of old constructions forming part of the cultural heritage, it is difficult to obtain these data by means of an experimental study because coring the existing structures of such buildings is rarely allowed. If it is allowed, it is restricted to very small quantities. It is thus necessary to choose the calculation parameters from a very small number of samples or from non-destructive tests carried out on site. In this context, it is particularly useful to know how to estimate the mechanical parameters from non-destructive tests such sonic tests (measurement of P-wave velocity, V_p) and the interval in which they usually vary.

For this reason, a database gathering together the mechanical parameters of 178 granites from many parts of the world was built up. Thanks to these data relating to a wide panel of granites, the existing relationships between physical parameters (ρ and V_p) and mechanical parameters (E, ν, f_c, f_t, ε_{peak}) could be studied.

We should point out that the word "granite", as used here, includes all the rocks identified under this name in the articles found in the international literature. Therefore, the term covers rocks with various chemical and mineralogical compositions. They were obtained from open quarries or by drilling at depth. The link between the mechanical properties, mineralogical nature and chemical composition of the rocks is not studied here (for analysis of the influence of the grain sizes and weathering grades, see [3] [4] [5] [11] [28] [30] [35] [36]). The aim of the present paper is to give an overall view of the mechanical properties of granite, wherever it may come from.

Section 2 of the paper recalls the key points concerning the mechanical behaviour of granite in the linear and non-linear domains, and the conclusions that some authors have drawn on this topic. The effects of the specimen size and the anisotropy of the materials are discussed. New tests were carried out recently on “Sidobre” granite (quarry in southern France) to enrich the database. They are presented in section 3. A synthetic description of the data collected is given in section 4. Finally, the database and the results of the new experimental campaign are considered together. The correlation relationships between physical and mechanical parameters are given in section 5.

2. Mechanical behaviour of granite in compression

Granites are rocks that are characterized by high mechanical strength - up to 220 MPa ([3] [15]) - and very low porosity [17].

Figure 1 recalls the different phases of the mechanical behaviour of granite in compression [10] [33]. It shows the typical relationships between the compressive stress and the longitudinal strain ε_L①, the transversal strain ε_T② and the volumetric strain $\frac{\Delta V}{V}$ ③, calculated using equation (1).

$$\frac{\Delta V}{V}=\varepsilon_L+2\varepsilon_T \qquad (1)$$

Curve ④ represents the variation of the volumetric strain of cracks. It was deduced from ③ after subtraction of $\left(\frac{\Delta V}{V}\right)_{el}$ given by equation (2).

$$\left(\frac{\Delta V}{V}\right)_{el}=\left(\frac{1-2\nu}{E}\right)\sigma \qquad (2)$$

The stresses f_{cc}, f_{ci}, f_{cd}, and f_c concern the following thresholds:

- f_{cc} : end of crack closure of pre-existing micro-cracks and beginning of linear increase of strains,
- f_{ci} : end of linear increase of transversal strain and beginning of crack opening,
- f_{cd} : beginning of damage with dilatancy,
- f_c : failure.

The points C, I and D are located as follows: point D is the maximum of curve ③. The portion CD of ① is linear. Point C is determined so as to follow the experimental curve ① optimally. Then, point I is positioned knowing that it is both at the end of the linear part of ② and at a change in slope of ③ (onset of cracking).

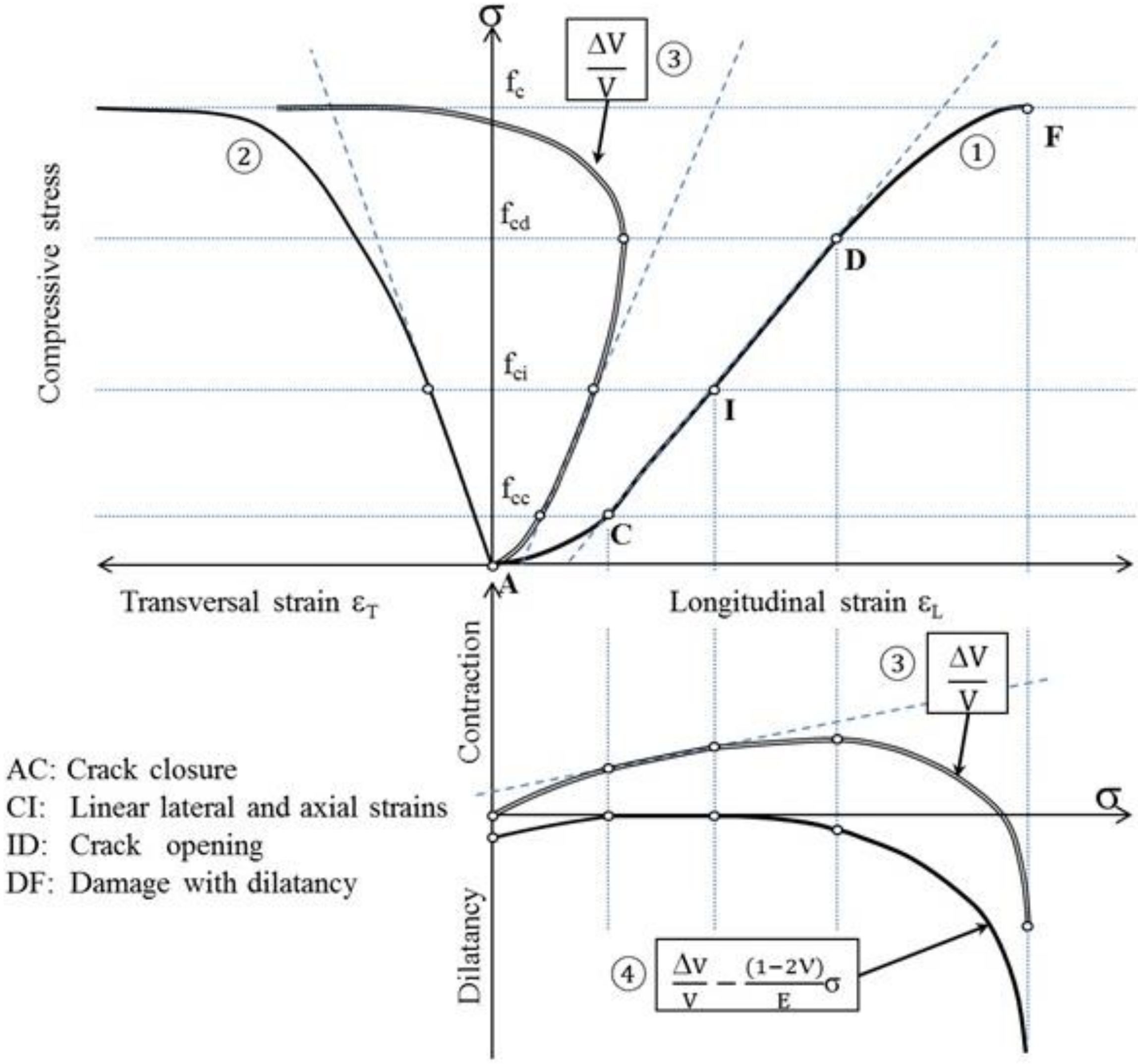

Fig.1 – Uniaxial compression test of granite. Typical stress/strain diagrams and changes in volume

Vasconcelos carried out a number of tests [33] on granites with a large range of compressive strengths, which were mostly collected from the northern region of Portugal (26-160 MPa). The elastic modulus varied from 11.1 GPa to 63.8 GPa. The Poisson's ratio values were in the interval 0.19-0.35 with a mean value of 0.28. She observed that, for low to medium strength granites, the values of f_{ci} were lower than $0.3f_c$, and, for high strength granite, the values lay in the interval $0.3\text{-}0.4f_c$. The ratio f_{cd}/f_c was about 0.7-0.8, in agreement with the measurements made by Eberhardt [10].

Effect of the specimen size

It is known that the experimental results of compression tests depend on the relation between the height, H, and the horizontal dimension, D, of the units. EN 772-1 (and so Eurocode 6) provides a form factor named δ for converting the test results $f_c(D,H)$ for a specimen of dimensions D,H, to those that would have been obtained for a specimen of dimensions (100 mm, 100 mm). The δ factor is recalled in Table 1. Linear interpolation is permitted. These coefficients will be used in section 4.

Table 1 – Form factor according EN 772-1

Height of unit (mm)	Smallest horizontal dimension of unit (mm)				
	50	100	150	200	250 or greater
50	0.85	0.75	0.7	-	-
65	0.95	0.85	0.75	0.7	0.65
100	1.15	1	0.9	0.8	0.75
150	1.3	1.2	1.1	1	0.95
200	1.45	1.35	1.25	1.15	1.1
250 or greater	1.55	1.45	1.35	1.25	1.15

Note that, according to Vasconcelos [31], the shape and size of the specimen do not significantly affect the value of the velocity of sound.

Effect of anisotropy

Granite may present a preferential planar orientation. The anisotropy, if it exists, can be detected by visual observation or using sonic tests, as the ultrasonic wave velocity is higher in the direction parallel to the foliation plane [31]. Unfortunately, in most articles consulted for the research presented here, the presence of anisotropy in the granite is not mentioned. Some authors, like Cerrillo [7], measure the anisotropy and conclude that it is low enough for granite to be regarded as an isotropic material. Due to the lack of precise information on this topic, anisotropy is not taken into account in this paper.

One can assume that the tests reported in the literature were carried out perpendicular to an orthotropy plane if such a plane was visible. In the event that the authors provide results in several loading directions, only results perpendicular to the foliation plane were saved in the database.

However, the importance of anisotropy should be relativized in the limited context of the research presented here, which aims to provide a global view of the mechanical characteristics of granite blocks embedded in old masonry structures, wherever and whenever they were built. The anisotropy of the granite blocks in masonry structures changes when cracks open and close according to the internal stresses. It is therefore different at each point of the structure and is evolving. At the macro-scale of a monument, the influence of the anisotropy of the masonry due to (i) cracking under loads and (ii) how the blocks are linked by horizontal and vertical mortar joints is much greater than the geological anisotropy of the granite blocks.

3. Experimental campaign on Sidobre granite

The region known as the Sidobre is located in the south of France, about 50 km east of Toulouse. This granitic massif extends over an area 16 km x 7 km. This granite has excellent ornamental and mechanical properties and was the subject of several scientific studies in the 20th century [4] [5] [17] [18] [25].

In the recent experimental campaign, 6 uniaxial compression tests were carried out, first on 100 mm x 100 mm x 100 mm cubes to estimate the uniaxial compressive strength, then on 6 cylindrical specimens, 50 mm in diameter and 100 mm high, to measure f_c, E and ν (see Figure 2). The set of results and the numerical values of the stress thresholds defined above are summarized in Table 2.

Fig.2 – Sidobre granite. Compressive test on cylindrical specimens, D=50 mm, H=100 mm

Table 2 - Sidobre granite test results. P-wave velocity, V_p; bulk density, ρ; and stress thresholds (SD = standard deviation, CV = coefficient of variation)

	Ultrasonic P-wave velocity	Bulk density	Compressive strength	Crack closure threshold	Cracking initiation threshold	Damage threshold
	V_p	ρ	f_c	f_{cc}	f_{ci}	f_{cd}
	m/s	10^3kg/m^3	MPa	MPa	MPa	MPa
A	5 051	2.703	180.7	23.6	76.9	118.0
B	4 608	2.571	142.4	18.8	66.5	110.2
C	4 490	2.675	148.4	10.5	59.1	110.3
D	4 679	2.592	160.9	16.9	56.0	105.2
E	4 389	2.652	157.2	18.0	59.5	109.1
F	4 532	2.729	160.9	12.0	63.1	124.0
Mean	**4 625**	**2.654**	**158.4**	**16.6**	**63.5**	**112.8**
SD	231	0.062	13.183	4.771	7.493	6.879
CV	5%	2%	8%	29%	12%	6%

The compressive strength obtained was f_c (100,100) = 186 MPa when using cubes (standard deviation = 7.6 MPa, 6 specimens) and f_c (50,100) = 158 MPa on 50 x 100 mm cylinders (standard deviation = 14.5 MPa, 6 specimens). Note that the f_c (100,100) / f_c (50,100) ratio was 1.17. This value is consistent with the coefficient of 1.15 specified by European standard EN 722-1 [37].

The stress-strain diagrams (longitudinal and transversal strains) up to failure are given in Figure 3. Figure 4 shows an example (specimen E, considered as the most representative) of cyclic loading test results (cycles up to $0.4f_c$, according to European standard EN14580 [41]).

The stress thresholds defined in section 2 were determined:

- Crack closure ended at a stress level around 10% of compressive strength f_c ($f_{cc}/f_c = 0.1$),
- Crack opening started when the stress was around 40% of f_c ($f_{ci}/f_c = 0.4$),
- Granite damage with dilatancy started at around 71% of f_c ($f_{cd}/f_c = 0.71$).

These results are in accordance with the results of Vasconcelos [33] and Eberhardt [10] for high strength granites, recalled in section 2.

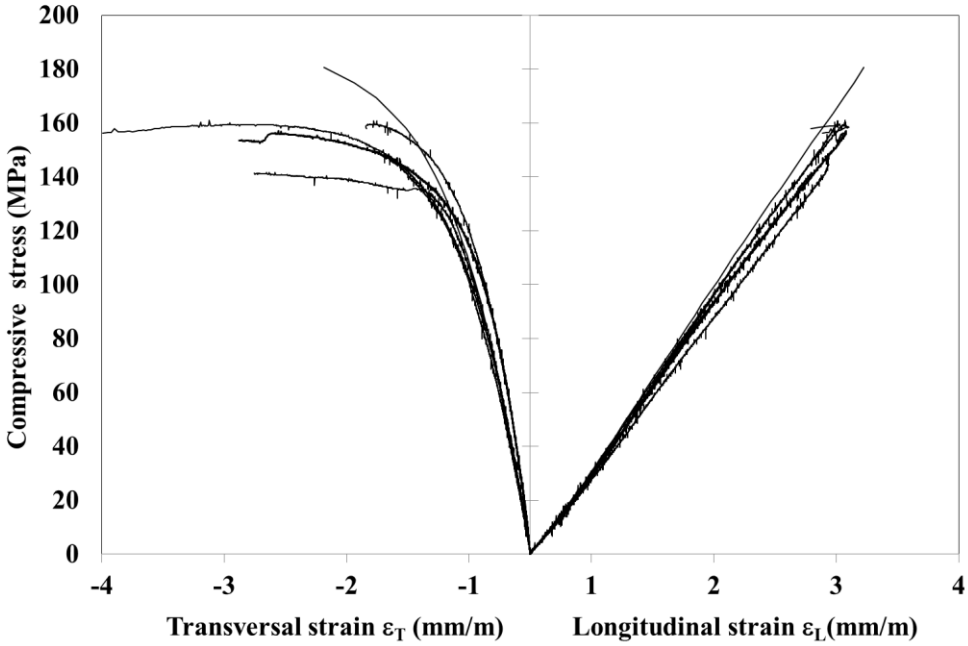

Fig.3 - Sidobre granite results. Stress-strain diagrams (cylindrical specimens 50 mm x 100 mm)

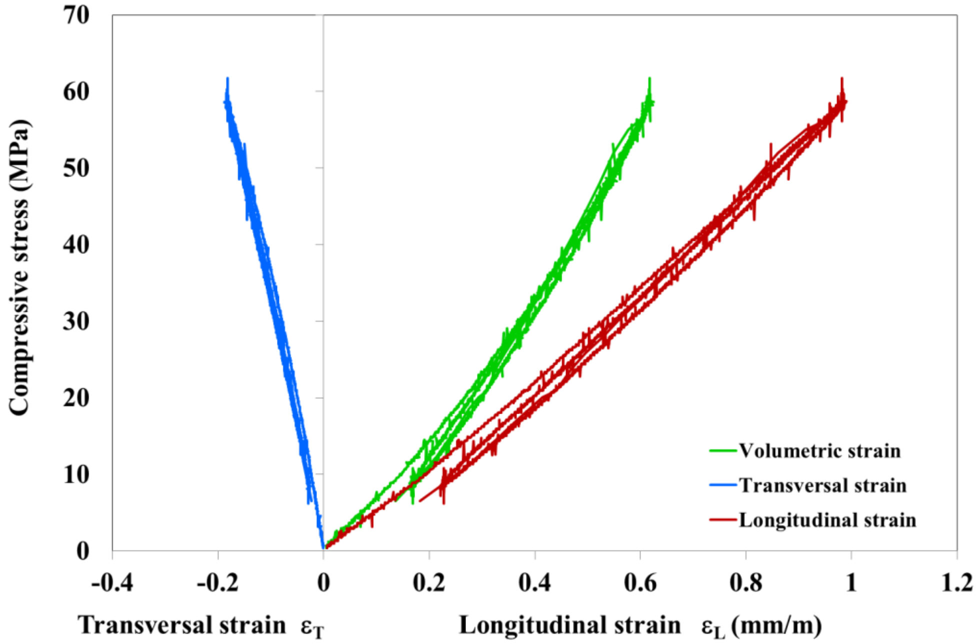

Fig.4 – Stress-strain curves with 3 loading-unloading cycles (specimen E)

Young's modulus

The linear phase of Sidobre granite is located between $0.1f_c$ and $0.4f_c$. According to European standard EN14580 [41], the Young's modulus has to be measured after 3 loading-unloading cycles between $0.02f_c$ and $0.2f_c$, and thus outside the linear phase found in the experimental study. Table 3 compares the slope values measured between C and I, between C and D, and according to EN 14580. It can be observed that the slopes measured are similar on the intervals C-I or C-D. The value of E obtained by applying standard EN14580 differs by 5%.

Table 3 - Sidobre granite results. Young's modulus and Poisson's ratio.

	Measurements between C and I		Measurements between C and D		According to EN 14580	
	E	ν	E	ν	E	ν
	GPa	-	GPa	-	GPa	-
A	67.8	0.299	68.0	0.350	71.8	0.282
B	64.7	0.273	62.7	0.321	67.0	0.274
C	59.4	0.260	58.9	0.315	62.1	0.262
D	65.3	0.271	66.2	0.343	67.8	0.267
E	64.2	0.211	63.4	0.282	66.5	0.204
F	65.9	0.215	65.0	0.296	68.6	0.212
Mean	**64.6**	**0.255**	**64.0**	**0.318**	**67.3**	**0.250**
SD	2.8	0.035	3.1	0.026	3.1	0.034
CV	4%	14%	5%	8%	5%	13%

Three-point bending tests

Flexural tensile tests were carried out on 6 specimens 50 mm x 50 mm x 300 mm. The average of experimental flexural tensile stress ($f_{ct,fl}$) was 12.8 MPa (CV=8%).

4. Data collection from the international literature

The database brought together results of experimental campaigns carried out between 1965 and 2014 on granites extracted in Europe (France [4] [5] [6] [13] [16] [17] [18] [21] [22] [24] [25] [26] [29], Portugal [27] [28] [31] [32] [33], Spain [1] [7]), Africa (Morocco [12]), Asia (Turkey [19] [30] [34] [35] [36], India [23], China [9]), South America [3] and North America [10][11]. It comprised 178 different granites, with an average of 5 samples tested per type of granite.
All authors provided the bulk density (ρ) and the uniaxial compressive strength (f_c) of the rocks they tested. The P-wave velocity (V_p), tensile strength (f_t), Young's modulus (E), Poisson's ratio (ν), strain at peak (ε_{peak}) and complete behaviour law were sometimes supplied.

Table 4 (physical parameters) and Table 5 (mechanical parameters) give a comprehensive and synthetic list of the data collected, parameter by parameter, including: the number of granites tested (N), minimum (Min), maximum (Max) and mean values (Mean), standard deviation (SD) and the coefficient of variation (CV = SD / Mean, in %). In Table 5, the values corresponding to direct tensile strength (f_{ct}), splitting tensile strength ($f_{ct,sp}$, Brazilian test) and flexural tensile strength ($f_{ct,fl}$, 3-point bending tests) are given separately.

Table 4 - Database – Physical parameters

	Porosity P_o %	P-wave velocity V_p m/s	Bulk density ρ $10^3 kg/m^3$
N	174	143	177
Min	0.06	2260	2.52
Max	5.06	6690	2.77
Mean	**0.75**	**4970**	**2.66**
SD	0.63	890	0.05
CV	84%	18%	2%

Table 5 - Database – Mechanical parameters

	Young's modulus E MPa	Poisson's ratio ν	Peak strain ε_{peak} mm/m	Compressive strength f_c MPa	Direct tensile strength f_{ct} MPa	Splitting tensile strength $f_{ct,sp}$ MPa	Flexural tensile strength $f_{ct,fl}$ MPa
N	77	65	18	178	19	44	72
Min	12900	0.14	1.2	54	1.8	3.1	7.0
Max	84969	0.34	5.4	236	11.4	28.0	28.3
Mean	**47613**	**0.25**	**2.9**	**138**	**4.8**	**15.5**	**15.2**
SD	16100	0.04	1.7	34	2.6	6.5	4.2
CV	34%	17%	59%	24%	55%	42%	28%

It can be observed from these tables (and Figure 6 below) that, while the compressive strength varies from about 54 to 236 MPa, the bulk density remains practically constant at 2.66± 2%. It appears that the bulk density, ρ, is not an indicator of compressive strength, f_c, as it is for calcareous stones, for example.

Histograms of f_c and V_p are presented in Figure 5.

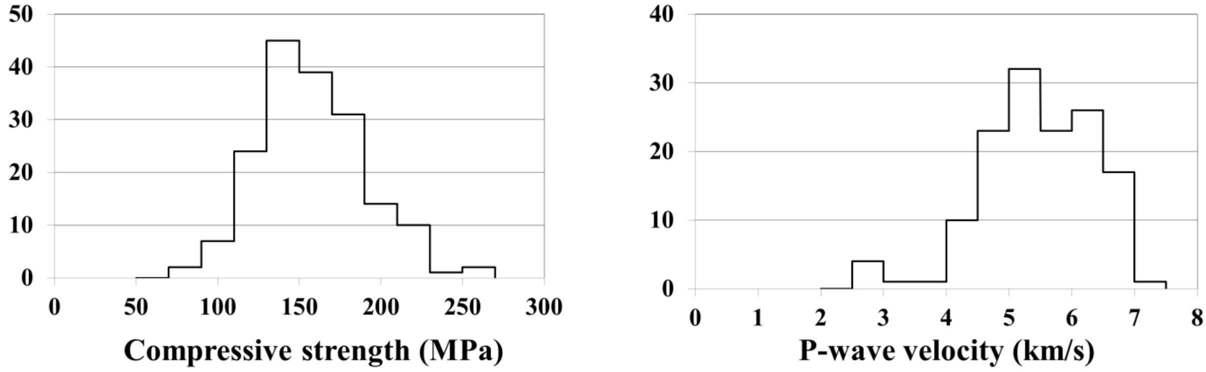

(a) (b)

Fig.5. Histograms of compressive strength f_c (a) and ultrasonic P-wave velocity V_p (b)

5. Relationships between parameters and correlations

The measurements collected in the database are presented below as curves showing how the physical and mechanical parameters are interrelated. Relationships including the compressive strength are presented first (Figures 6 to 10), then those including tensile strength. (Figures 11 to 13). The authors are mentioned in the legend of each figure. Each point represents a type of granite (i.e. granite mined from a given quarry). It is therefore the average of all the values provided by the authors for one geographical site (average of 3 to 30 tests per point, depending on the authors). The new tests carried out on Sidobre granite have been added with the reference "LMDC" (Laboratoire Matériaux et Durabilité des Constructions). Each curve corresponds to one of the 7 correlation relationships given in Table 6. They were obtained by minimizing the error between experimental and theoretical values (least-squares method), taking account of the number of tests assigned to each point. For this calculation, a normal distribution of the populations around the mean value was assumed (permitted by the histograms shown in Figure 5). In the Figures, the correlation laws are drawn in continuous lines and the 90% confidence interval is shown in dotted lines. By considering all the figures, it can be seen that the error margin is largest for the most resistant granite.

Table 6. Correlation relationships

Parameters	Correlation laws	R^2	Figure
f_c (MPa) - P_o (%)	$f_c = 154.9\ e^{-0.21Po}$	0.35	7
f_c (MPa) –V_p (km/s)	$f_c = 46.95\ Vp^{0.68}$	0.27	8
E (MPa) - f_c (MPa)	$E = 340.2\ f_c$	0.66	9
ν - f_c (MPa)	$\nu = 0.27$	0.26	10
f_{cd} (MPa) - f_c (MPa)	$f_{cd}=0.050f_c^{1.531}$	0.982	11
f_{ci} (MPa) - f_c (MPa)	$f_{ci}=0.083f_c^{1.29}$	0.937	11
f_t (MPa) - f_c (MPa)	$f_t=0.123f_c$	0.45	13

5.1. Relationships with compressive strength f_c

Figures 6 to 10 show the following relationships: f_c vs ρ (Fig.6), f_c vs P_o (Fig.7), f_c vs V_p (Fig.8), E vs f_c (Fig.9), and ν vs f_c (Fig.10), where f_c is the compressive strength after application of "K", to take account of the effect of the specimen sizes. The authors selected, and listed in the References section, followed different recommendations when carrying out their tests (ISRM suggested methods (1981c) [20], ASTM [2], or European standards [37]) and so used different sizes of specimens. In order to make comparisons among the results, it was necessary to weight each value of the database by a scale factor, named K here. It was decided to take the dimensions of a cylinder having a diameter, D, of 50 mm and a height, H, of 100 mm as the reference. "K" values given by equation (3), and listed in Table 7, were calculated by linear interpolation from the values provided by EN 772-1 [37] and recalled in section 2. Recent tests carried out on Sidobre granite, and reported in section 3, confirmed the validity of the coefficients.

$$K=\frac{f_c(50,100)}{f_c(D,H)} \qquad (3)$$

with:

$f_c(50,100)$: Mean strength of a cylindrical specimen with D =50 mm and H=100 mm,
$f_c(D,H)$: Mean strength of a cylindrical specimen with other values of D and H.

Table 7 - Coefficient K

D (mm)	H (mm)	H/D	K
40	40	1	0.71
50	50	1	0.74
54	54	1	0.75
70	70	1	0.79
20	40	2	0.90
36	72	2	0.95
50	100	2	1
50	123	2.46	1.06
68	140	2.06	1.06
75	150	2	1.09

Figure 6 shows the relationship between the compressive strength, fc, and the bulk density. As mentioned in the previous section, the density varied very little around the mean value (2660 kg/m^3). This is why no correlation is proposed for this figure. It can simply be seen that the point cloud is narrow.

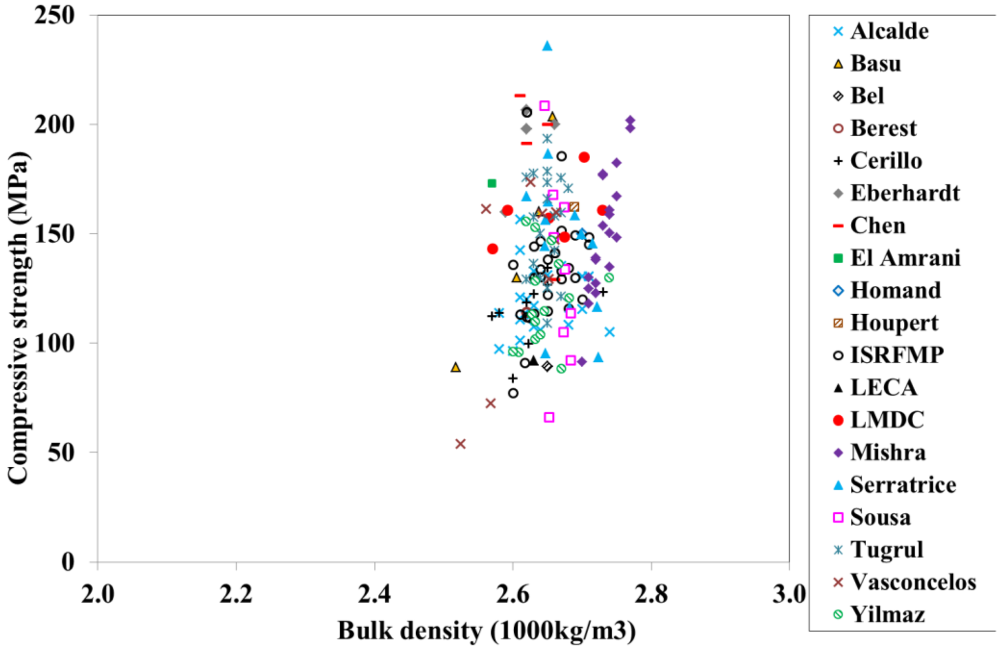

Fig.6. Compressive strength, f_c, versus bulk density, ρ

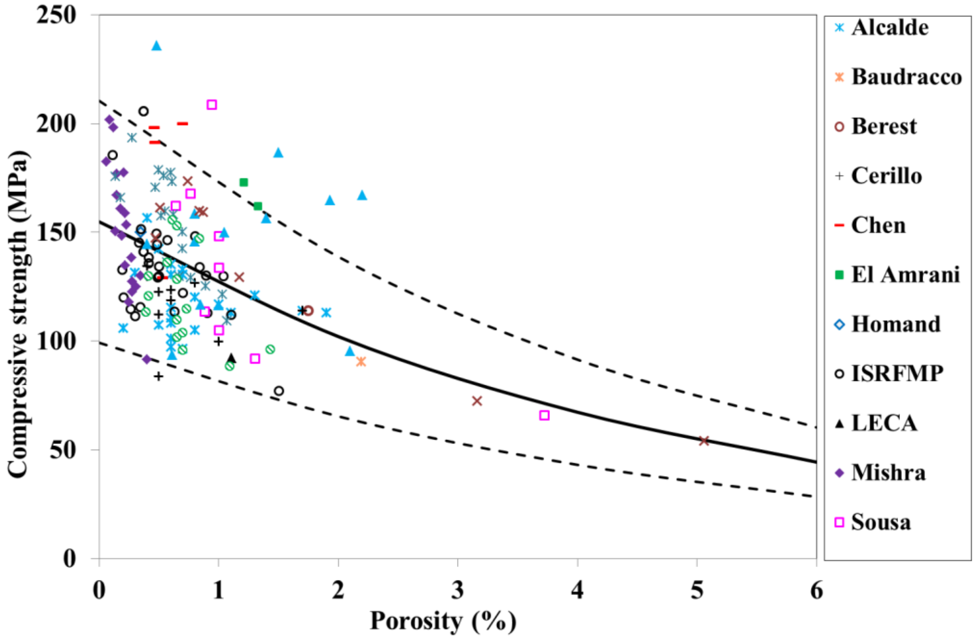

Fig.7. Compressive strength, $f_{c,}$ versus porosity, P_o

In Figure 7, the point cloud is almost exclusively located in the area Po <1.5%. It is obvious that the compressive strength f_c decreases as the porosity increases (Figure 7). This is due to micro-cracks. These micro-cracks explain the variation of f_c with the ultrasonic P-wave velocity (Figure 8). As Pérami [25] already reported in 1965, the ultrasonic P-wave velocity V_p in a rock depends on its cracking state and its elastic properties. Its measurement provides a good indication of the rock quality. Sixteen authors used this technique on granite with frequency ranges from 50 Hz to 200 Hz. As shown by Vasconcelos [31], the frequency variations induced very little variation in the velocity measured. So, the results can be compared without distinction on the frequency used. The results are shown in Figure 8. The correlation relationships of Tugrul [30] and Vasconcelos [31] (similar to those of Souza [28]) have been added. These relationships are perfectly suited to the granite of a given geographical area but are not valid elsewhere. The correlation relationship proposed for the entire database crosses these at their mean value.

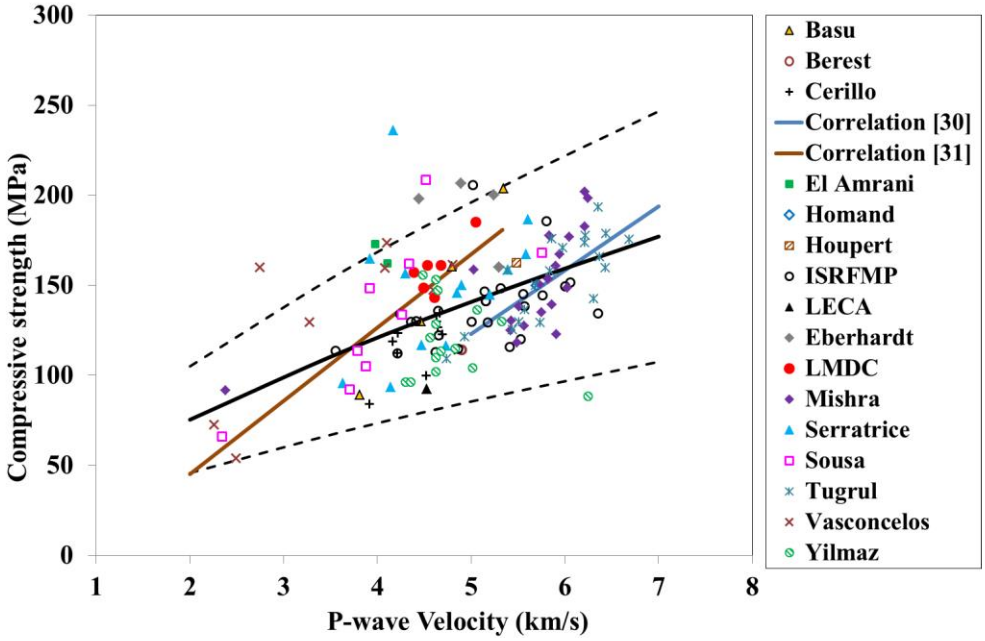

Fig.8. Compressive strength, f_c, versus P-wave velocity, V_p

As can be seen in Figure 9, the modulus of elasticity, E, can be estimated from the compressive strength, f_c, with a linear function. The E/f_c ratio for all the granite of the database is 340. The slopes of the correlation relationships proposed for some granite from Portugal [33] and Turkey [30] are slightly different but remain within the 90% confidence interval.

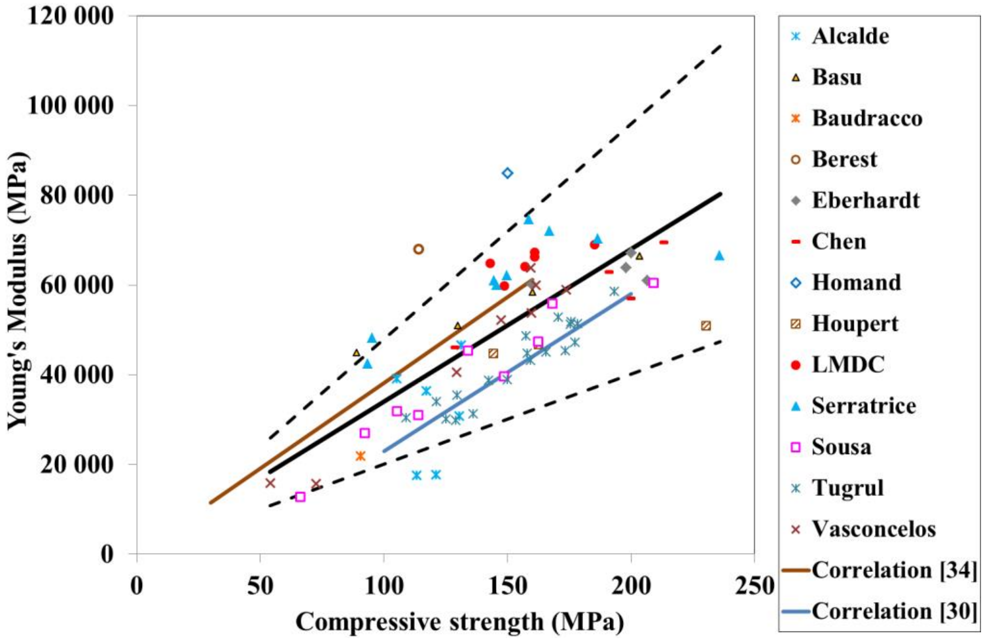

Fig.9. Young's modulus, E, versus compressive strength, f_c

Fig. 10 shows that, overall, the Poisson's ratio does not vary with the compressive strength of the material. The correlation relationship is a horizontal line corresponding to $\nu = 0.27$.

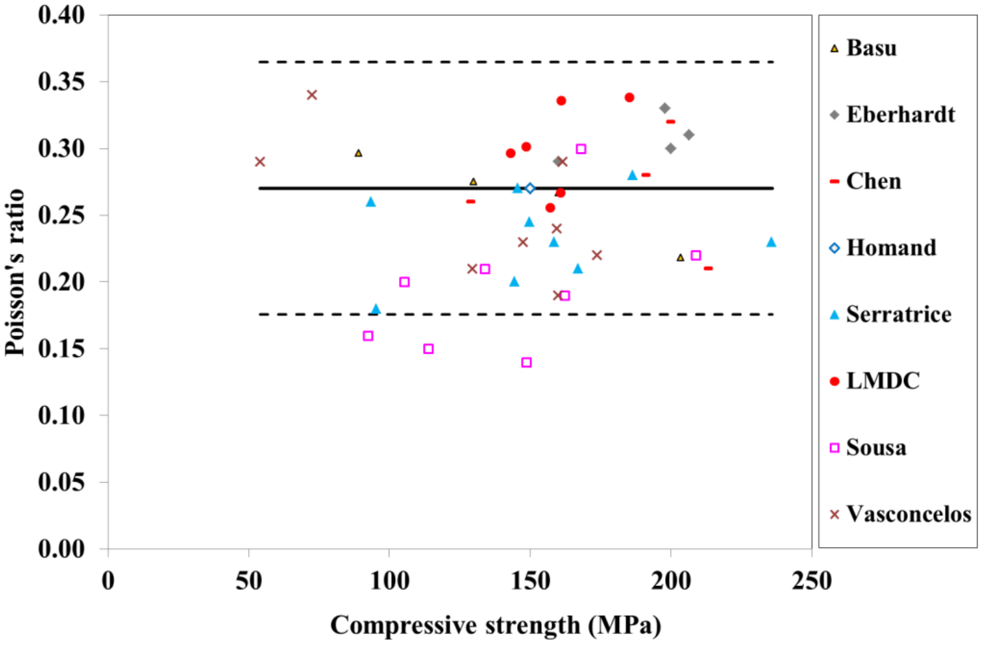

Fig.10. Poisson's ratio, ν, versus compressive strength, f_c

Relationship between f_{ci}, f_{cd} and f_c

Figure 11 describes the relationship between the crack initiation threshold f_{ci}, then the damage threshold f_{cd}, and the compressive strength, f_c, for Sidobre granite and the results found by two other authors [33] [10]. The results agree. Each cloud of points falls within a narrow interval, giving the good correlation presented above.

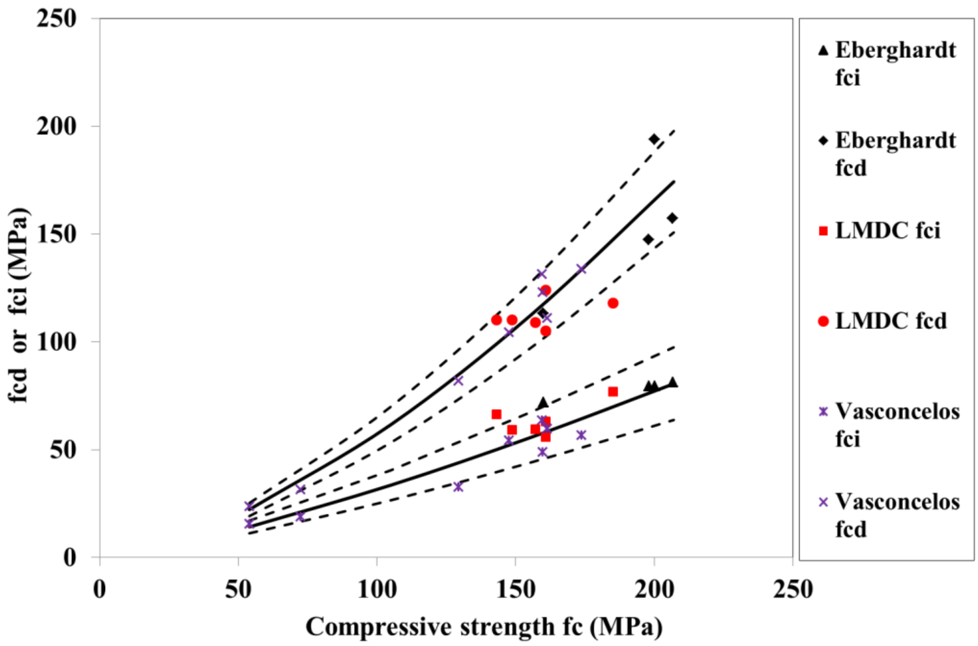

Fig.11 – Variation of f_{cd} and f_{ci} with the compressive strength f_c

5.2. Relationships with tensile strength f_t

In the articles referenced, the mean value of "f_t" in the tensile tests is 13.2 MPa (CV 46%), about one tenth of the mean value of the compressive strength f_c (50,100). However, the tensile strength was measured according to 3 different experimental methods, depending on the authors: direct tensile test (f_{ct}), splitting tensile test ($f_{ct,sp}$), or 3-point bending test ($f_{ct,fl}$). For a given type of granite, the results differ depending on the procedure. But how? To answer this question, Figure 12 shows the tensile test results coloured according to the method used so as to distinguish the 19 direct tensile tests, the 44 Brazilian tensile tests and the 72 three-point bending tests found in the literature. LMDC tests on Sidobre granite have been added.

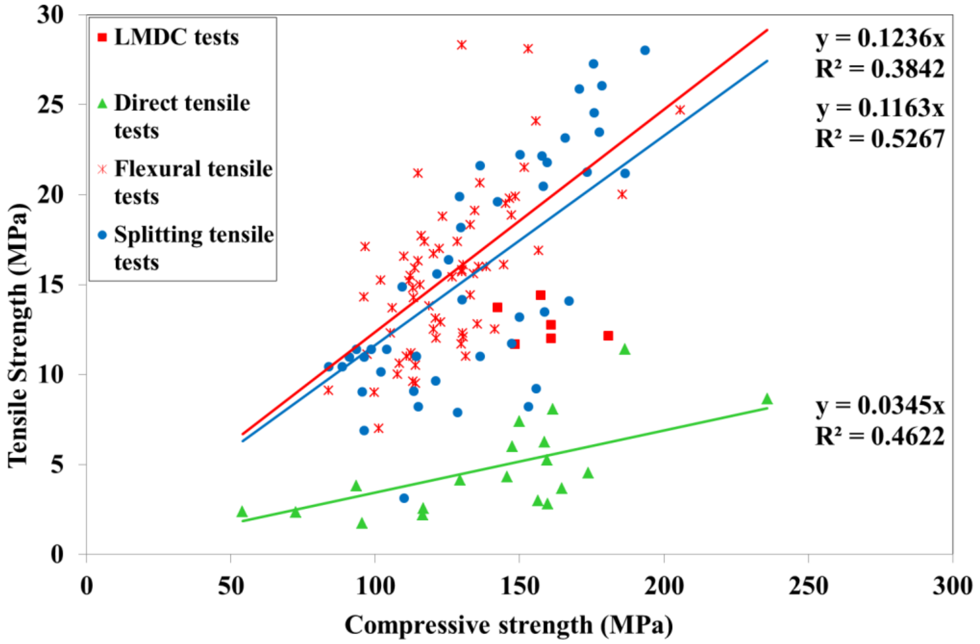

Fig.12. Tensile strength versus compressive strength, f_c, according to type of test

The clouds of points for the last two types of tests (splitting and flexural tests) are superimposed, while the direct tensile tests gave significantly lower values than the other two. Table 8 shows the average of compressive and tensile strengths obtained according to the type of test. Bending and splitting tests gave a similar "f_c/f_t" ratio (8.4 and 8.8) while f_c differed by 5%, 5 times less than the coefficient of variation corresponding to f_c. The ratios $f_{ct,fl}$ / f_{ct} and $f_{ct,sp}$ / f_{ct} were around 3.

Table 8 – Comparison between tensile tests according to type of test

	Direct tensile strength f_{ct} (MPa)	Splitting tensile strength $f_{ct,sp}$ (MPa)	3-point bending strength $f_{ct,fl}$ (MPa)
N	19	44	72
f_c (MPa)	140.9	135.5	128.0
f_t (MPa)	4.8	15.5	15.2
f_c / f_t	29.6	8.8	8.4

Unfortunately, there were not enough comparative studies to enable a formula to be found for passing from one test to another in an accurate and realistic way. However, this experimental observation indicates that it is not possible to mix the results of the 3 test procedures without taking account of the gap observed. Thus, in order to compare the results of tensile tests, all results were transformed to the value that would have been obtained in 3-point bending tests, by applying a coefficient of 3 to direct tensile tests, and keeping the results of splitting tests as they were. The resulting curve (f_{ct} – f_c) is presented in Figure 13. The overall average of the tensile test results obtained is 15.7 MPa (CV = 33%), so about 0.12 f_c. Note that this ratio is significantly higher than those of Serratine [26] for both sandstone and granite (0.08) but lower than those of Tugrul [30]. The correlation relationships proposed by these two authors are reported in Figure 13. They are both in the 90% confidence interval around the correlation relationship proposed here.

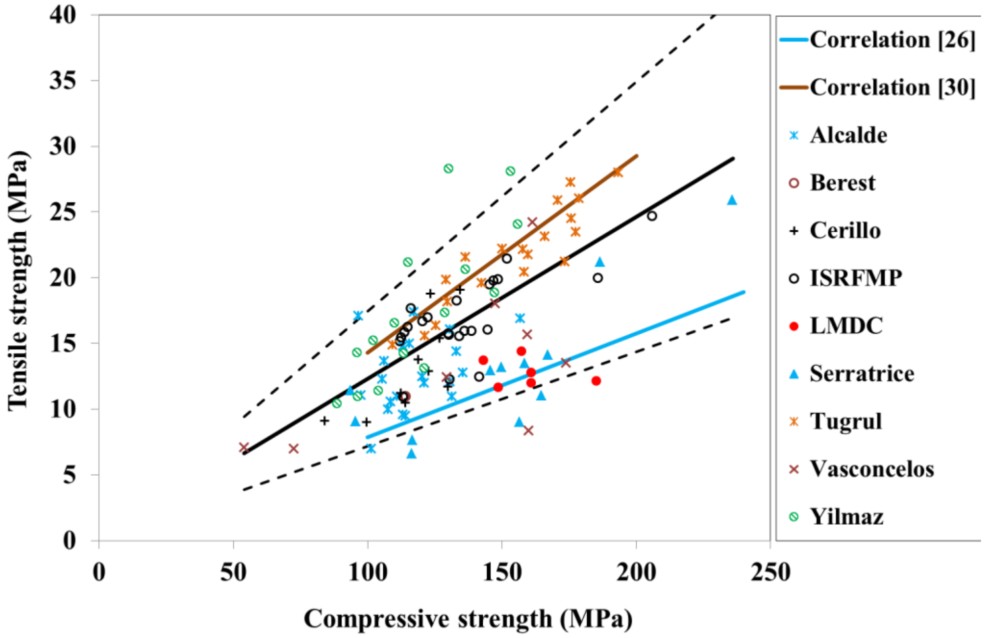

Fig.13. Tensile strength, f_{ct}, versus compressive strength, f_c.

6. Conclusions

A database gathering together the mechanical properties of 178 granites was built up from international scientific research published between 1965 and the present day. Large variability was observed in the measured parameters with a large dispersion of the results, except for the bulk density, which was almost constant and equal to 2660 ± 2% kg/m^3. So, the bulk density of granite is not an indicator of its compressive strength (f_c).

An experimental campaign carried out on granite from southern France has been presented and added to the database. This rock has a compressive strength of about 158 MPa, which is 15% above the mean value of all the granites included in the database (138 MPa). Its mechanical behaviour under uniaxial compression load presents the following successive steps:
- At the beginning of the loading and up to 0.10f_c, the cracks close,
- Then, cracks open above 0.4 f_c,
- Granite damage with dilatancy starts at around 0.71 f_c.

In the linear part of the mechanical behaviour, the experimental Young's modulus of Sidobre granite is 64 GPa. The European standard gives 67 GPa, 5% more, because the stress interval imposed extends beyond the linear zone.

In order to aid engineers and researchers in the determination of mechanical parameters, 7 correlation relationships between physical parameters (bulk density ρ, porosity P_o, P-wave velocity V_p) and mechanical parameters (f_c, f_{ct}, E, ν) have been proposed, taking account of the effect of the specimen sizes. In the future, these relationships will allow the mechanical parameters of granite to be estimated from ultrasonic measurements, in a 90% confidence interval. It can be noted, in particular, that the relation between Young's Modulus and compressive strength is linear (E = 340f_c), and the Poisson's ratio is constant at around 0.27. Some authors have proposed correlation relationships in the past. They were precise and accurate for granite from a limited region. The advantage of the correlation relationships presented here is that they cover a wide variety of granite from around the world.

Acknowledgements
The authors would like to thank the ISRFMP, “Institut Supérieur de Recherche et de Formation aux Métiers de la Pierre”, for free access to their rocks database, and M. Plo, director of the Sidobre quarry “Carrières PLO” for supplying granite free of charge.

References

[1] Alcalde Molero C., Perianes A., Consejeria de economia y trabajo de la junta de extremadura. Atlas de las rocas ornamentales de Extremadura, Spain, 2004.

[2] ASTM D7012-14, Standard Test Methods for Compressive Strength and Elastic Moduli of Intact Rock Core Specimens under Varying States of Stress and Temperatures, ASTM International, West Conshohocken, PA, 2014.

[3] Basu A., Celestino T.B., Bortolucci A. Evaluation of rock mechanical behaviors under uniaxial compression with reference to assessed weathering grades. Rock Mechanics and Rock Engineering (2009) 42: 73-93.

[4] Baudracco J., Bel M., Pérami R., Effets de l’altération sur quelques propriétés mécaniques du granite du Sidobre. Bulletin de l’association international d’ingénierie et géologie n°25, 33-38, Paris, 1982.

[5] Bel M., Modalités de l'altération du granite du Sidobre : conséquences sur diverses propriétés mécaniques, PhD Thesis, Université de Toulouse, 1974.

[6] Berest P., Charpentier J.P., Habib P. Étude du comportement mécanique d'un granite sous contrainte et température élevées. Sciences et techniques nucléaires. CECA-CEE-CEEA, Brussels, Luxembourg, 1985.

[7] Cerrillo C., Jiménez A., Rufo M., Paniagua J., Pachón F.T. New contributions to granite characterization by ultrasonic testing. Ultrasonics 54 (2014) 156–167.

[8] Charrier K., Domède N. Inventer une poutre en pierre précontrainte. Rapport de recherche, Laboratoire Matériaux et Durabilité des Constructions, Toulouse, June 2014.

[9] Chen Y., Hu S., Wei K., Hu R., Zhou C., Jing L. Experimental characterization and micromechanical modeling of damage-induced permeability variation in Beishan granite. International Journal of Rock Mechanics & Mining Sciences 71 (2014) 64-76.

[10] Eberhardt E., Stead D., Stimpson B., Read R.S. Identifying crack initiation and propagation thresholds in brittle rock. Can. Geotech. J; Vol. 35 (1998) 222-233.

[11] Eberhardt E., Stimpson B., Stead D. Effects of grain size on the initiation and propagation thresholds of stress-induced brittle fractures. Rock mechanics and rock engineering. 32 (1999) 81-99.

[12] El Amrani El Hassani I.E., El Azhari H. Evaluation des propriétés physico-mécaniques des pierres de construction du Maroc à partir des vitesses des ondes P et de la résistance au choc. Bulletin de l’Institut Scientifique, Rabat, section Sciences de la Terre 31 (2009) 41-54.

[13] Fourmaintraux D. Quantification des discontinuités de la roche et du massif rocheux, Méthodes et applications. Bulletin de liaison du laboratoire des Ponts et Chaussées 75 (1975) 69-76.

[14] Gardner G.H.F., Gardner L.W., Gregory A.R. Formation velocity and density, the diagnostic basics for stratigraphic traps. Geophysics 39 (1974) 770-780.

[15] Habib P. An outline of soil and rock mechanics, Cambridge University Press, 1983.

[16] Homand F., Chiarelli AS., Caractéristiques physiques et mécaniques du granite de la Vienne et de l'argilite de l'Est, Revue Française de Génie civil, 6 (2002) 12-20.

[17] Houpert R. Comportement mécanique des roches cristallines à structure quasi isotrope. PhD Thesis, University of Toulouse, 1973.

[18] Houpert R., Tisot J.P. Effet d'échelle et dispersion des contraintes de rupture en compression simple dans le cas d'un granite. 2ème colloque sur la fissuration des roches, Revue de l'industrie minérale, 14 January 1969.

[19] Kahraman S. Evaluation of simple methods for assessing the uniaxial compressive strength of rock. International Journal of Rock Mechanics & Mining Sciences 38 (2001) 981–994.

[20] ISRM Suggested Methods. Rock characterization, testing and monitoring, Pergamon Press: Oxford, 1981. (1981c).

[21] ISRFMP, Institut Supérieur de Recherche et de Formation aux métiers de la Pierre, Mémoire de Pierre, CD ROM database 1999.

[22] Leca D. Caractérisation des altérations du granite d'Auriat (Creuse). Etude de son espace poreux. PhD Thesis. Ecole Nationale des Ponts et Chaussées, France, 1990.

[23] Mishra D.A., Basu A. Estimation of uniaxial compressive strength of rock materials by index tests using regression analysis and fuzzy inference system. Engineering Geology 160 (2013) 54–68.

[24] Panet M., Fourmaintraux D. La mécanique des roches appliquée aux ouvrages du génie civil, Ecole Nationale des Ponts et Chaussées. France, Aix-en-Provence, 1976.

[25] Pérami R. Sur la formation de micro discontinuités dans les roches sous l'effet de la compression simple, applications géotechniques. PhD Thesis, University of Toulouse, 1965.

[26] Serratrice JF., Durville JL. Description des roches et des massifs rocheux. Exploitation de deux bases de données. Bulletin des laboratoires des Ponts et Chaussées, 211 (1997) 73-87.

[27] Sousa L.M.O., Suárez del Río L.M., Calleja L., Ruiz de Argandona V.G., Rey A.R. Influence of microfractures and porosity on the physico-mechanical properties and weathering of ornamental granites. Engineering Geology 77 (2005) 153–168.

[28] Sousa L.M.O. Petrophysical properties and durability of granites employed as building stone: a comprehensive evaluation. Bull Eng Geol Environ (2014) 73:569–588.

[29] Tourenq C., Denis A. La résistance à la traction des roches, rapport de recherché n°4, Ministère de l'équipement et du logement, Laboratoire des Ponts et Chaussées, France, February 1970.

[30] Tugrul A., Zarif I.H. Correlation of mineralogical and textural characteristics with engineering properties of selected granitic rocks from Turkey. Engineering Geology 51 (1999) 303–317.

[31] Vasconcelos G., Lourenço P.B., Alvez C.A.S., Pamplona J. Ultrasonic evaluation of the physical and mechanical properties of granites. Ultrasonics 48 (2008) 453-466.

[32] Vasconcelos G., Experimental investigations on the mechanics of stone masonry: Characterization of granites and behavior of ancient masonry shear walls. PhD thesis, University of Minho, 2005.

[33] Vasconcelos G., Lourenço, P. B. Experimental characterization of the compressive behavior of granites. Mecanica Experimental, 2008, Vol 16, pp. 61-71.

[34] Yasar E., Erdogan Y. Correlating sound velocity with density, compressive strength and Young's modulus of carbonate rocks. International Journal of Rock Mechanics & Mining Sciences 41 (2004) 871-875.

[35] Yilmaz N.G., Mete Goktan R., Kibici Y. Relations between some quantitative petrographic characteristics and mechanical strength properties of granitic building stones. International Journal of Rock Mechanics & Mining Sciences 48 (2011) 506–513.

[36] Yilmaz N.G., Karaca Z., Goktana R.M., Akal C. Relative brittleness characterization of some selected granitic building stones: Influence of mineral grain size. Construction and Building Materials 23 (2009) 370–375.

[37] EN 772-1. Methods of test for masonry units. Determination of compressive strength (2011)

[38] EN 1936. Natural stone test methods. Determination of real density and apparent density and of total and open porosity (2006)

[39] EN 12372. Natural stone test methods. Determination of flexural strength under concentrated load (2007)

[40] EN 14579. Natural stone test methods. Determination of sound speed propagation (2005)

[41] EN 14580. Natural stone test methods. Determination of static elastic modulus (2005)